communications physics

Article

https://doi.org/10.1038/s42005-024-01605-w

Coulomb exchange as source of Kitaev and off-diagonal symmetric anisotropic couplings

Pritam Bhattacharyya [1] ✉, Thorben Petersen[1], Nikolay A. Bogdanov [2] & Liviu Hozoi[1] ✉

Exchange underpins the magnetic properties of quantum matter. In its most basic form, it occurs through the interplay of Pauli's exclusion principle and Coulomb repulsion, being referred to as Coulomb or direct exchange. Pauli's exclusion principle combined with inter-atomic electron hopping additionally leads to kinetic exchange and superexchange. Here we disentangle the different exchange channels in anisotropic Kitaev–Heisenberg context. By quantum chemical computations, we show that anisotropic Coulomb exchange, completely neglected so far in the field, may be as large as (or even larger than) other contributions — kinetic exchange and superexchange. This opens new perspectives onto anisotropic exchange mechanisms and sets the proper conceptual framework for further research on tuning Kitaev–Heisenberg magnetism.

Magnetism has constantly been a source of new fundamental concepts in solid-state and statistical physics. It is also important to technological applications: many devices around us are (electro)magnetic. Magnetism is typically illustrated through Heisenberg's textbook model of interacting atomic magnetic moments. Recently, however, it has become clear that for certain magnetic materials Heisenberg's isotropic interaction picture is not applicable; their behavior can only be described through highly *anisotropic* spin models. The latter may imply completely different interaction strengths for different magnetic-moment projections and, seemingly counterintuitive, directional dependence of the leading anisotropic coupling[1–3] for symmetry-equivalent pairs of moments. While that opens entire new perspectives in magnetism, provides the grounds for new, exotic states that are now being revealed for the first time, and hints to potential technological applications like quantum computation[1], how such anisotropies arise is not yet fully clarified: we know those may be dominant in particular systems but do not understand in detail the underlying physics and how to tune such interactions in the lab.

Here we shed fresh light on the exchange mechanisms underlying symmetric anisotropic magnetic interactions, both diagonal (i.e., Kitaev[1,2]) and off-diagonal, by using ab initio quantum chemical computational methods. To do so, we exploit the ladder of controlled approximations that quantum chemistry offers: single-configuration schemes, multi-configuration theory, and multireference configuration-interaction. Honeycomb α-$RuCl_3$, in particular, the relatively high-symmetry crystalline structure recently discovered under a pressure of $\approx$1.3 GPa[4], and triangular-lattice $NaRuO_2$[5] were chosen as benchmark Kitaev–Heisenberg material platforms. We establish that a decisive contribution to the Kitaev effective coupling constant K comes from (anisotropic) Coulomb exchange, a mechanism ignored so far in the literature. In the case of the off-diagonal (x-z/y-z) interaction Γ', which can give rise to spin liquid ground states by itself[6], anisotropic Coulomb exchange is even dominant, as much as ~90% of the effective coupling parameter computed by multireference configuration-interaction. Our analysis provides unparalleled specifics as concerns t_{2g}^5–t_{2g}^5 Kitaev–Heisenberg magnetic interactions and perspective onto what reliable quantitative predictions would imply: not only controlled ab initio approximations to explicitly tackle intersite virtual excitations but also exact Coulomb exchange; the latter is available in self-consistent-field Hartree–Fock theory, the former in post–Hartree–Fock wave-function-based quantum chemical methods.

Results

Kitaev magnetism refers to anisotropic magnetic interactions $K\tilde{S}_i^\gamma\tilde{S}_j^\gamma$ that are 'bond' dependent, i.e., for a given pair of adjacent 1/2 pseudospins $\tilde{\mathbf{S}}_i$ and $\tilde{\mathbf{S}}_j$, the easy axis defined through the index γ can be parallel to either x, y, or z[1]. This can be easily visualized for layered configurations of edge-sharing ML_6 octahedra derived from the rocksalt crystalline arrangement (see Fig. 1), either triangular-lattice AMO_2[3,7] or honeycomb A_2MO_3[2] (and MCl_3) structures, where M, A, and L are transition-metal, alkaline, and ligand ions, respectively: for each of the magnetic 'bonds' emerging out of a given magnetic site M, the easy axis (x, y, or z) is normal to the square plaquette defined by two adjacent transition ions and the two bridging ligands. Kitaev's honeycomb spin model has quickly become a major reference point

[1]Institute for Theoretical Solid State Physics, Leibniz IFW Dresden, Helmholtzstraße 20, Dresden 01069, Germany. [2]Max Planck Institute for Solid State Research, Heisenbergstraße 1, Stuttgart 70569, Germany. ✉e-mail: pritambhattacharyya01@gmail.com; l.hozoi@ifw-dresden.de

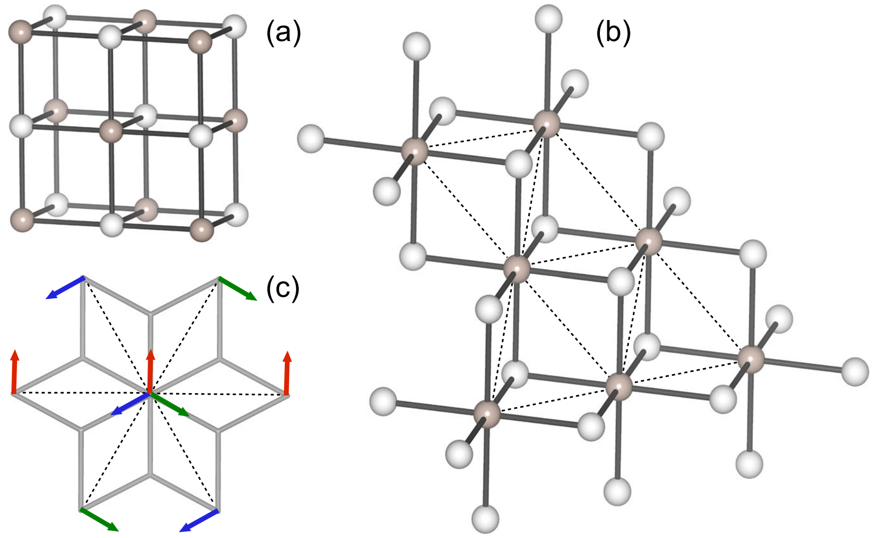

Fig. 1 | Orthogonal M_2L_2 plaquettes in rocksalt structure and derivatives. a Rocksalt-type lattice. The M-L bonds are along either *x*, *y*, or *z*. **b** With two different cation species (*A*, *B*) forming successive layers normal to the [111] axis, a rhombohedral ABL_2 structure is realized—each layer features a triangular network of edge-sharing octahedra. Honeycomb A_2BL_3 structures are obtained when one of the cation species (*A*) occupies additional sites within the layer of the other (*B*), corresponding to the centers of B_6 hexagonal rings; in α-$RuCl_3$, all *A* sites are empty. **c** On each B_2L_2 plaquette (ions not drawn), the Kitaev interaction couples only spin components normal to the respective plaquette. All three spin projections are shown only for the central magnetic site.

in quantum magnetism research: it is exactly solvable and yields a quantum spin liquid (QSL) ground state in which the spins fractionalize into emergent Majorana quasiparticles[1]. The latter are neutral self-adjoint fermions that are simultaneously particle and antiparticle. QSL ground states have been proposed for the Kitaev–Heisenberg honeycomb systems $H_3LiIr_2O_6$[8] and α-$RuCl_3$[9,10] and also in a triangular-lattice magnet with seemingly sizable anisotropic intersite couplings, $NaRuO_2$[5]. However, in the case of the honeycomb compounds, what is described as QSL behavior either occurs in the presence of coupling-parameter disorder induced by unavoidable randomness of the H^+ cations ($H_3LiIr_2O_6$) or requires an external magnetic field (α-$RuCl_3$).

Having QSL phases materialized on both hexagonal and triangular networks of Ru_2L_2 plaquettes makes Ru quite special. For insights into t_{2g}^5–t_{2g}^5 anisotropic exchange in both α-$RuCl_3$ and $NaRuO_2$ crystallographic settings, detailed quantum chemical calculations were carried out for Ru_2Cl_{10} and Ru_2O_{10} magnetic units as found in the respective materials. The adjacent in-plane RuL_6 octahedra coordinating those two-octahedra central units were also explicitly included in the quantum chemical computations but using more compact atomic basis sets. The finite quantum mechanical cluster was embedded within a large array of point changes which reproduces the crystalline Madelung field within the cluster volume. To generate this collection of point charges we employed the EWALD package[11,12]. Complete-active-space self-consistent-field (CASSCF) optimizations[13,14] were initially performed with six (Ru t_{2g}) valence orbitals and ten electrons as active (abbreviated hereafter as (10e,6o) active space). Subsequently, two other types of wave-functions were generated, using in each case the orbitals obtained from the (10e,6o) CASSCF calculations: (i) single-configuration (SC) t_{2g}^5–t_{2g}^5 (i.e., the t_{2g}^4–t_{2g}^6 and t_{2g}^6–t_{2g}^4 configurations which were accounted for in the initial CASSCF were excluded in this case by imposing appropriate orbital-occupation restrictions) and (ii) multireference configuration-interaction (MRCI)[13,15] wave-functions having the (10e,6o) CASSCF as kernel and additionally accounting for single and double excitations out of the central-unit Ru t_{2g} and bridging-ligand valence *p* (either O 2*p* or Cl 3*p*) orbitals. By comparing data at these different levels of approximation—SC, CASSCF, and MRCI—it is possible to draw conclusions on the role of various exchange mechanisms. The CASSCF optimization was performed for the lowest nine singlet and lowest nine triplet states associated with the (10e,6o) setting. Those were the states for which spin-orbit couplings (SOCs) were further accounted for[16], at either SC, CASSCF, or MRCI level, which yields in each case a number of 36 spin-orbit states.

A unit of two nearest-neighbor octahedra exhibits C_{2h} point-group symmetry, in both α-$RuCl_3$[4] and $NaRuO_2$[5], implying a generalized bilinear effective spin Hamiltonian of the following form for a pair of adjacent 1/2-pseudospins $\tilde{\mathbf{S}}_i$ and $\tilde{\mathbf{S}}_j$:

$$\mathcal{H}_{ij}^{(\gamma)} = J\tilde{\mathbf{S}}_i \cdot \tilde{\mathbf{S}}_j + K\tilde{S}_i^{\gamma}\tilde{S}_j^{\gamma} + \sum_{\alpha\neq\beta}\Gamma_{\alpha\beta}(\tilde{S}_i^{\alpha}\tilde{S}_j^{\beta} + \tilde{S}_i^{\beta}\tilde{S}_j^{\alpha}). \quad (1)$$

The $\Gamma_{\alpha\beta}$ coefficients denote the off-diagonal components of the 3×3 symmetric-anisotropy exchange tensor, with $\alpha,\beta,\gamma\in\{x,y,z\}$. The lowest four spin-orbit eigenstates from the ab initio quantum chemical output (eigenvalues lower by ~ 0.2 eV with respect to the eigenvalues of higher-lying excited states) are mapped for each different set of calculations onto the eigenvectors of the effective spin Hamiltonian (1), following the procedure described in refs. 17,18: those four expectation values and the matrix elements of the Zeeman Hamiltonian in the basis of the four lowest-energy spin-orbit eigenvectors are put in direct correspondence with the respective eigenvalues and matrix elements of (1).

Nearest-neighbor effective magnetic couplings as obtained at three different levels of theory (SOC included) for α-$RuCl_3$ under pressure are listed in Table 1. A very interesting finding is the vanishingly small *J* value in the spin-orbit MRCI computations. This yields a fully anisotropic *K*-Γ-Γ′ effective model for the nearest-neighbor magnetic interactions and in principle increases the chances of realizing a QSL ground state, compared to the system at ambient pressure. In the latter case, magnetic field is needed to induce QSL behavior[9,10].

Even more remarkable are the large anisotropic Coulomb exchange contributions obtained by SC calculations with SOC. The diagonal Kitaev coupling *K*, for example, is basically the same at the lowest two levels of approximation (first column in Table 1), SC (only the t_{2g}^5–t_{2g}^5 electron configuration considered) and CASSCF (10e,6o) (t_{2g}^5–t_{2g}^5, t_{2g}^4–t_{2g}^6, and t_{2g}^6–t_{2g}^4 configurations treated on the same footing, where the latter type of states bring kinetic Ru (t_{2g})–Ru(t_{2g}) exchange). This indicates that intersite Ru (t_{2g}) → Ru (t_{2g}) excitations (i.e., kinetic exchange) do not really affect *K*.

Table 1 | Nearest-neighbor magnetic couplings (meV) in high-symmetry α-$RuCl_3$[4], results of spin-orbit calculations at various levels of theory

	K	*J*	$\Gamma_{xy}\equiv\Gamma$	$\Gamma_{yz}=\Gamma_{zx}\equiv\Gamma'$
SC	−1.75	0.35	−0.11	0.42
CASSCF (10e,6o)	−1.73	−1.04	0.89	0.46
MRCI	−3.73	−0.03	1.62	0.45

The MRCI is performed having the (10e,6o) CASSCF wave-function as kernel.

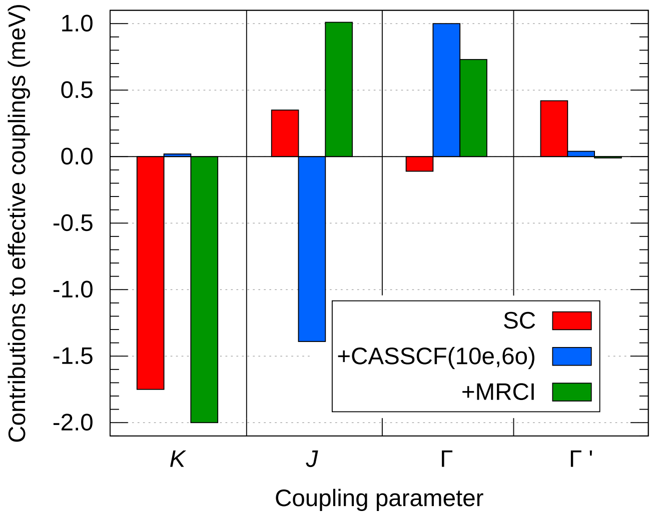

Fig. 2 | Exchange contributions to the intersite effective magnetic couplings in high-symmetry α-$RuCl_3$[4]. Coulomb exchange (single-configuration (SC) results, in red), Ru(t_{2g})--Ru(t_{2g}) kinetic exchange (as the difference between complete-active-space self-consistent-field (CASSCF) and SC data, in blue), plus contributions related to Ru(t_{2g}) → Ru(e_g) excitations[2,3,19], Ru-Cl_2-Ru superexchange[2,3,19–21], and so called dynamical correlation effects[13] (as the difference between multireference configuration-interaction (MRCI) and CASSCF, in green).

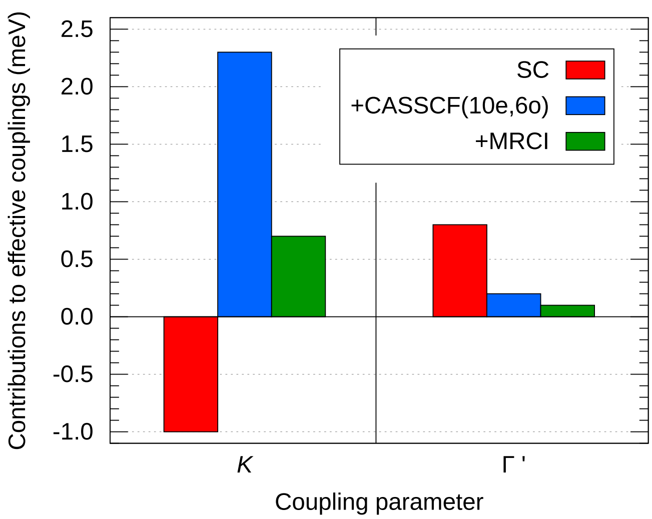

Fig. 3 | Exchange contributions to K and Γ′ in $NaRuO_2$[5]. Coulomb exchange (single-configuration (SC) results, in red), Ru(t_{2g})--Ru(t_{2g}) kinetic exchange (as the difference between complete-active-space self-consistent-field (CASSCF) and SC data, in blue), plus contributions related to Ru(t_{2g}) → Ru(e_g) intersite excitations, Ru-O_2-Ru superexchange, and dynamical correlations (as the difference between multireference configuration-interaction (MRCI) and CASSCF, in green).

What matter as concerns the size of the Kitaev coupling are (i) Coulomb exchange, with a contribution of −1.75 meV, and (ii) Ru-Cl_2-Ru superexchange[2,3,19–21], excitations involving the Ru 4*d* e_g levels[2,3,19], and so called dynamical correlation effects[13] accounted for by MRCI, with a combined contribution of −2 meV. Especially striking is the diagnosis carried out for the off-diagonal Γ′ effective interaction parameter: out of a spin-orbit MRCI value of 0.45 meV, 0.42 corresponds to anisotropic Coulomb exchange. A pictorial representation of the various contributions to *K*, *J*, Γ, and Γ′ in high-symmetry α-$RuCl_3$[4] is provided in Fig. 2.

MRCI+SOC computations for adjacent edge-sharing RuO_6 octahedra in triangular-lattice $NaRuO_2$ indicate that the largest nearest-neighbor coupling parameter is the isotropic Heisenberg *J*, −5.2 meV; the other effective interactions, *K*, Γ, and Γ′, amount to 2, 3.6, and 1.1 meV, respectively, by spin-orbit MRCI. For better visualization, since the most important anisotropic Coulomb exchange contributions arise also in this system for *K* and Γ′, we depict in Fig. 3 only the structure of these two magnetic couplings and omit the *J* and Γ effective interactions, which have significantly larger absolute values. Plots for the latter are provided in Supplementary Fig. 1. It is seen that anisotropic Coulomb exchange represents again the second largest contribution to the Kitaev *K* and the leading underlying mechanism in the case of Γ′. Interestingly, for *K* and *J*, adding the Coulomb-exchange contributions obtained by SC quantum chemical calculations (−1.0 and −0.7 meV, respectively) to estimates obtained from effective-model (super)exchange theory ($K = 2.9$ and $J = -4.2$ meV)[22], brings the latter in rather good agreement with the MRCI+SOC values (2.0 and −5.2 meV, respectively), although this is not the case for Γ and Γ′.

Discussion

Anisotropic Coulomb exchange as found in the SC calculations (also referred to as direct exchange[20] in isotropic context or potential exchange) has been mentioned as possibly relevant player in Dzyaloshinskii–Moriya cuprate context[23] but not addressed in existing Kitaev–Heisenberg literature (see, e.g., the effective-model studies of refs. 19,22,24–27). Finding that up to ~45% of the Kitaev effective coupling constant *K* has to do with Coulomb exchange and that the off-diagonal anisotropic coupling Γ′, which may give rise to spin-liquid ground states by itself[6], comes more than 90% from Coulomb exchange (last column in Table 1) obviously challenges present views and notions in Kitaev–Heisenberg quantum magnetism research. This is just another example illustrating the need for ab initio quantum chemical methods in order to achieve even a qualitatively correct picture of the essential underlying physics. Recent quantum chemical results that lead to the same conclusion refer to the role of fluctuations involving the third and fourth electronic shells in renormalizing antiferromagnetic interactions in copper oxide compounds[28].

To provide additional reference points, we computed the isotropic Coulomb exchange integrals (i.e., without accounting for SOC) for different distributions of the Ru t_{2g} holes in SC t_{2g}^5–t_{2g}^5 arrangement (see Supplementary Table 1). For holes in plaquette-plane 4*d* orbitals having overlapping lobes along the Ru-Ru axis (i.e., for *xy*-like t_{2g} functions), for example, the Coulomb exchange integral amounts to −25.4 meV. For comparison, in 3d^9 copper oxide compounds, the Coulomb exchange matrix element lies in the region of −4 meV for edge-sharing geometry[29] and −10 meV for corner-sharing ligand octahedra[30,31] (from SC $d^1_{x^2-y^2}$–$d^1_{x^2-y^2}$ calculations). For the latter type of linkage, being aware of experimental estimates of 100–250 meV for the Heisenberg *J*, an isotropic Coulomb exchange contribution of −10 meV can be neglected. But this is not the case for edge-sharing octahedra, in either Ru or Cu compounds.

How exactly SOC and Coulomb interactions commix to yield large *anisotropic* Coulomb exchange integrals remains to be analyzed in detail in future work. The important point however is that, at the SC (t_{2g}^5–t_{2g}^5) level, there is a Coulomb exchange matrix element for each possible pair of holes —d_{xy}-d_{xy}, d_{xy}-d_{yz} etc. SOC mixes up those different Slater determinants, and the resulting spin-orbit wave-functions are not spin eigenstates. Additionally, spin-orbit interactions remove the degeneracy of the 'triplet' states in the two-site magnetic problem. The spin-orbit fine structure in the two-site magnetic problem can be reduced to an effective pseudospin model only by introducing anisotropic Coulomb exchange matrix elements (i.e., the SC values provided in Table 1).

To summarize, we resolve the exchange mechanisms giving rise to anisotropic magnetic interactions on hexagonal and triangular networks of edge-sharing RuL_6 t_{2g}^5 octahedra. Different from present assumptions and models relying exclusively on inter-atomic hopping (i.e., on *indirect* exchange), the quantum chemical analysis indicates major *direct* exchange contributions, to both *K* and Γ′. This redefines the conceptual frame within which anisotropic intersite interactions should be addressed. In light of the ab initio quantum chemical data, various estimates, interpretations, and predictions based only on kinetic-exchange and superexchange mechanisms might require reevaluation—what is represented in red color in Figs. 2 and 3 is simply ignored in existing effective-model theories and studies. Our findings provide solid reference points for reliable electronic-structure investigations of other, closely related t_{2g}^5 Kitaev materials and also of $t_{2g}^5 e_g^2$ $j \approx 1/2$ magnets.

Methods

All quantum chemical computations were carried out with the MOLPRO suite of programs[32]. Atomic coordinates as determined by Stahl et al.[4] and Ortiz et al.[5] were used for α-$RuCl_3$ and $NaRuO_2$, respectively. We employed energy-consistent relativistic pseudopotentials (ECP28MDF) and Gaussian-type valence basis sets (BSs) of effective quadruple-ζ quality (ECP28MDF-VTZ)[33] for the 'central' Ru species. All-electron BSs of quintuple-ζ quality were utilized for the two bridging ligands (Cl[34] in α-$RuCl_3$ and O[35] in $NaRuO_2$) and of triple-ζ quality for the remaining eight anions[34,35] linked to the two octahedra of the reference, cental unit. The four adjacent cations in α-$RuCl_3$ and eight adjacent transition ions in $NaRuO_2$ were represented as closed-shell Rh^{3+} t_{2g}^6 species, using Ru ECP29 pseudopotentials and [3s3p3d] Ru BSs[33] from the MOLPRO library. The outer 16 Cl ligands associated with the four adjacent octahedra in α-$RuCl_3$ and the outer 22 O ligands associated with the eight adjacent octahedra in $NaRuO_2$ were described through minimal atomic-natural-orbital (ANO) BSs[36]. Large-core pseudopotentials were considered for the 22 Na nearby cations[37] in $NaRuO_2$.

We used the standard coordinate frame usually employed in the literature, different from the rotated frame employed in earlier quantum chemical studies[18,38,39] that affects the sign of Γ (see also footnote [48] in ref. 40). The SC label in Table I in the main text indicates a CASCI in which intersite excitations are not considered. This is also referred to as occupation-restricted multiple active space (ORMAS) scheme[41].

Data availability

Quantum chemical data (input atomic coordinates, point charge embeddings, MOLPRO outputs) on which this manuscript is based are publicly available.

Code availability

Relevant codes are available from the corresponding author upon reasonable request.

Received: 30 December 2023; Accepted: 22 March 2024;
Published online: 08 April 2024

References

1. Kitaev, A. Anyons in an exactly solved model and beyond. *Ann. Phys.* **321**, 2–111 (2006).
2. Jackeli, G. & Khaliullin, G. Mott insulators in the strong spin-orbit coupling limit: from Heisenberg to a quantum compass and Kitaev models. *Phys. Rev. Lett.* **102**, 017205 (2009).
3. Khaliullin, G. Orbital order and fluctuations in Mott insulators. *Prog. Theor. Phys. Supp.* **160**, 155 (2005).
4. Stahl, Q. et al. Pressure-tuning of α-$RuCl_3$ towards the ideal Kitaev-limit. arXiv:2209.08367 (2022).
5. Ortiz, B. R. et al. Quantum disordered ground state in the triangular-lattice magnet $NaRuO_2$. *Nat. Phys.* **19**, 943–949 (2023).
6. Rousochatzakis, I. & Perkins, N. B. Classical spin liquid instability driven by off-diagonal exchange in strong spin-orbit magnets. *Phys. Rev. Lett.* **118**, 147204 (2017).
7. Reitsma, A. J. W., Feiner, L. F. & Oleś, A. M. Orbital and spin physics in $LiNiO_2$ and $NaNiO_2$. *N. J. Phys.* **7**, 121 (2005).
8. Kitagawa, K. et al. A spin–orbital-entangled quantum liquid on a honeycomb lattice. *Nature* **554**, 341–345 (2018).
9. Banerjee, A. et al. Neutron scattering in the proximate quantum spin liquid α-$RuCl_3$. *Science* **356**, 1055–1059 (2017).
10. Baek, S.-H. et al. Evidence for a field-induced quantum spin liquid in α-$RuCl_3$. *Phys. Rev. Lett.* **119**, 037201 (2017).
11. Klintenberg, M., Derenzo, S. E. & Weber, M. J. Accurate crystal fields for embedded cluster calculations. *Comp. Phys. Commun.* **131**, 120–128 (2000).
12. Derenzo, S. E., Klintenberg, M. K. & Weber, M. J. Determining point charge arrays that produce accurate ionic crystal fields for atomic cluster calculations. *J. Chem. Phys.* **112**, 2074–2081 (2000).
13. Helgaker, T., Jørgensen, P. & Olsen, J. *Molecular Electronic Structure Theory* (John Wiley & Sons, 2000).
14. Kreplin, D. A., Knowles, P. J. & Werner, H.-J. MCSCF optimization revisited. ii. combined first- and second-order orbital optimization for large molecules. *J. Chem. Phys.* **152**, 074102 (2020).
15. Knowles, P. J. & Werner, H.-J. Internally contracted multiconfiguration-reference configuration interaction calculations for excited states. *Theor. Chim. Acta* **84**, 95–103 (1992).
16. Berning, A., Schweizer, M., Werner, H.-J., Knowles, P. J. & Palmieri, P. Spin-orbit matrix elements for internally contracted multireference configuration interaction wavefunctions. *Mol. Phys.* **98**, 1823–1833 (2000).
17. Bogdanov, N. A. et al. Orbital reconstruction in nonpolar tetravalent transition-metal oxide layers. *Nat. Commun.* **6**, 7306 (2015).
18. Yadav, R. et al. Kitaev exchange and field-induced quantum spin-liquid states in honeycomb α-$RuCl_3$. *Sci. Rep.* **6**, 37925 (2016).
19. Chaloupka, J., Jackeli, G. & Khaliullin, G. Kitaev-Heisenberg model on a honeycomb lattice: possible exotic phases in iridium oxides A_2IrO_3. *Phys. Rev. Lett.* **105**, 027204 (2010).
20. Anderson, P. W. New approach to the theory of superexchange interactions. *Phys. Rev.* **115**, 2–13 (1959).
21. Kanamori, J. Superexchange interaction and symmetry properties of electron orbitals. *J. Phys. Chem. Solids* **10**, 87–98 (1959).
22. Razpopov, A. et al. A $j_{\rm eff} = 1/2$ Kitaev material on the triangular lattice: the case of $NaRuO_2$. *npj Quantum Mater.* **8**, 36 (2023).
23. Yildirim, T., Harris, A. B., Aharony, A. & Entin-Wohlman, O. Anisotropic spin Hamiltonians due to spin-orbit and Coulomb exchange interactions. *Phys. Rev. B* **52**, 10239 (1995).
24. Rau, J. G., Lee, E. K.-H. & Kee, H.-Y. Generic spin model for the honeycomb iridates beyond the Kitaev limit. *Phys. Rev. Lett.* **112**, 077204 (2014).
25. Yamaji, Y., Nomura, Y., Kurita, M., Arita, R. & Imada, M. First-principles study of the honeycomb-lattice iridates Na_2IrO_3 in the presence of strong spin-orbit interaction and electron correlations. *Phys. Rev. Lett.* **113**, 107201 (2014).
26. Winter, S. M., Li, Y., Jeschke, H. O. & Valentí, R. Challenges in design of Kitaev materials: magnetic interactions from competing energy scales. *Phys. Rev. B* **93**, 214431 (2016).
27. Winter, S. M. et al. Models and materials for generalized Kitaev magnetism. *J. Phys. Condens. Matter* **29**, 493002 (2017).
28. Bogdanov, N. A., Manni, G. L., Sharma, S., Gunnarsson, O. & Alavi, A. Enhancement of superexchange due to synergetic breathing and hopping in corner-sharing cuprates. *Nat. Phys.* **18**, 190–195 (2022).
29. Matsuda, M. et al. Highly dispersive magnons with spin-gap-like features in the frustrated ferromagnetic $S = \frac{1}{2}$ chain compound $Ca_2Y_2Cu_5O_{10}$ detected by inelastic neutron scattering. *Phys. Rev. B* **100**, 104415 (2019).
30. Martin, R. L. Cluster studies of La_2CuO_4: a mapping onto the Pariser-parr-people (PPP) model. *J. Chem. Phys.* **98**, 8691–8697 (1993).
31. van Oosten, A. B., Broer, R. & Nieuwpoort, W. C. Heisenberg exchange enhancement by orbital relaxation in cuprate compounds. *Chem. Phys. Lett.* **257**, 207–212 (1996).
32. Werner, H.-J., Knowles, P. J., Knizia, G., Manby, F. R. & Schütz, M. Molpro: a general-purpose quantum chemistry program package. *WIREs Comput. Mol. Sci.* **2**, 242–253 (2012).

33. Peterson, K. A., Figgen, D., Dolg, M. & Stoll, H. Energy-consistent relativistic pseudopotentials and correlation consistent basis sets for the 4*d* elements Y–Pd. *J. Chem. Phys.* **126**, 124101 (2007).
34. Woon, D. E. & Dunning Jr, T. H. Gaussian basis sets for use in correlated molecular calculations. iii. the atoms aluminum through argon. *J. Chem. Phys.* **98**, 1358–1371 (1993).
35. Dunning, T. H. Gaussian basis sets for use in correlated molecular calculations. i. The atoms boron through neon and hydrogen. *J. Chem. Phys.* **90**, 1007–1023 (1989).
36. Pierloot, K., Dumez, B., Widmark, P.-O. & Roos, B. O. Density matrix averaged atomic natural orbital (ANO) basis sets for correlated molecular wave functions. *Theor. Chim. Acta* **90**, 87–114 (1995).
37. Fuentealba, P., Preuss, H., Stoll, H. & Von Szentpály, L. A proper account of core-polarization with pseudopotentials: single valence-electron alkali compounds. *Chem. Phys. Lett.* **89**, 418–422 (1982).
38. Nishimoto, S. et al. Strongly frustrated triangular spin lattice emerging from triplet dimer formation in honeycomb Li_2IrO_3. *Nat. Commun.* **7**, 10273 (2016).
39. Yadav, R. et al. Engineering Kitaev exchange in stacked iridate layers: impact of inter-layer species on in-plane magnetism. *Chem. Sci.* **10**, 1866–1872 (2019).
40. Janssen, L., Andrade, E. C. & Vojta, M. Magnetization processes of zigzag states on the honeycomb lattice: Identifying spin models for $RuCl_3$ and Na_2IrO_3. *Phys. Rev. B* **96**, 064430 (2017).
41. Ivanic, J. Direct configuration interaction and multiconfigurational self-consistent-field method for multiple active spaces with variable occupations. I. method. *J. Chem. Phys.* **119**, 9364 (2003).

Acknowledgements
We thank J. Geck, S. D. Wilson, G. Khaliullin, S. Winter, O. Janson, U. K. Rößler, S. L. Drechsler, and R. C. Morrow for discussions. P.B., T.P., and L.H. acknowledge financial support from the German Research Foundation (Deutsche Forschungsgemeinschaft, DFG), projects 441216021 and 468093414, and technical assistance from U. Nitzsche.

Author contributions
P.B. performed the ab initio quantum chemical computations and subsequent analysis, with assistance from L.H., N.A.B., and T.P.; P.B. and L.H. wrote the paper, with contributions from the other coauthors.

Funding
Open Access funding enabled and organized by Projekt DEAL.

Competing interests
The authors declare no competing interests.

Additional information
Supplementary information The online version contains supplementary material available at https://doi.org/10.1038/s42005-024-01605-w.

Correspondence and requests for materials should be addressed to Pritam Bhattacharyya or Liviu Hozoi.

Peer review information *Communications Physics* thanks the anonymous reviewers for their contribution to the peer review of this work. A peer review file is available.